Contribution from the Department of Chemistry, University of Houston, Houston, Texas 77204-5641, and Laboratoire de Synthèse et d'Electrosynthèse Organométallique, associé au CNRS (URA 33), Université de Bourgogne, Faculté des Sciences "Gabriel", 6, Boulevard Gabriel, 21100 Dijon, France

Electrochemical and Spectroelectrochemical Studies of Tin(II) Porphyrins

K. M. Kadish,*[1a] D. Dubois,[1a] J.-M. Barbe,[1b] and R. Guilard*[1b]

Received March 19, 1991

The first electrochemistry of four-coordinate Sn(II) porphyrins is reported. The investigated compounds are represented as (P)Sn where P is the dianion of octaethylporphyrin (OEP), tetra-*p*-tolylporphyrin (TpTP), tetra-*m*-tolylporphyrin (TmTP), or tetramesitylporphyrin (TMP). Each complex undergoes two one-electron reductions in pyridine (py), tetrahydrofuran (THF), or benzonitrile (PhCN) containing 0.1 M tetrabutylammonium perchlorate, $(TBA)ClO_4$, or tetrabutylammonium hexafluorophosphate, $(TBA)PF_6$, as supporting electrolyte. The first reduction occurs in the range −1.05 to −1.40 V, while the second is located at −1.47 to −1.85 V vs SCE, depending upon the specific porphyrin ring. Both electrode reactions involve the porphyrin π ring system. The oxidation of (P)Sn was also investigated in the three solvents and gave $[(P)Sn^{IV}(S)(X)]^+$ (where S = py, THF, or PhCN and X = PF_6^- or ClO_4^-) as a final product of an irreversible two-electron transfer. A transient Sn(IV) product was also observed in pyridine or tetrahydrofuran on the electrochemical time scale. This species is postulated to be the bis-solvated $[(P)Sn(S)_2]^{2+}$ species and undergoes two reductions, which occur at −0.13 to −0.40 and −0.50 to −0.89 V vs SCE.

Introduction

Numerous group 14 metalloporphyrins have been synthesized[2-4] and studied with respect to their electrochemical,[3-8] photochemical,[9,10] and biological properties.[13,14] Most investigated derivatives contain a central metal ion in the +4 oxidation state, but tin (II)[9,15] and lead (II)[16,17] metalloporphyrins are also known. These latter compounds have not been studied in great detail, and it was not until recently that pure samples of (P)Sn derivatives (where P is a given porphyrin ring) have become available for characterization.[18]

Low-valent tin porphyrins are good precursors for the synthesis of new Sn(IV) derivatives, and this was recently demonstrated for the case of (P)SnS and (P)SnSe.[19] It was therefore of interest to investigate the electrooxidation and electroreduction of these four-coordinate Sn(II) porphyrins under conditions similar to those used for studying the electron-transfer reactions of five- and six-coordinate Sn(IV) porphyrins with halide[8] or chalcogen[19] axial ligands or five-coordinate Sn(II) porphyrin derivatives of the type $(P)SnFe(CO)_4$.[20] This is done in the present study, which characterizes the oxidation and reduction of $(P)Sn^{II}$ where P is the dianion of octaethylporphyrin (OEP), tetra-*p*-tolylporphyrin (TpTP), tetra-*m*-tolylporphyrin (TmTP), or tetramesitylporphyrin (TMP).

Experimental Section

Chemicals. Each (P)Sn derivative was prepared according to literature procedures[18] and then stored in a Vacuum Atmospheres glovebox under an inert atmosphere. Pyridine (py) and tetrahydrofuran (THF) were distilled over calcium hydride, while benzonitrile (PhCN) was distilled on P_2O_5. All solvents were thoroughly degassed with O_2-free Ar prior to use. Tetrabutylammonium hexafluorophosphate, $(TBA)PF_6$, was purchased from Fluka and twice recrystallized from ethyl acetate. Tetrabutylammonium perchlorate, $(TBA)ClO_4$, was purchased from Kodak and twice recrystallized from absolute ethanol. Both supporting electrolytes were dried in a vacuum oven at 40 °C prior to use.

Instrumentation. All experiments were carried out in a Vacuum Atmospheres glovebox except for those involving use of the Tracor Northern 6500 rapid-scan spectrometer. Cyclic voltammograms were recorded with a three-electrode system using an IBM EC 225 voltammetric analyzer which was connected to a Houston Instruments Model 2000 X-Y recorder or with a BAS 100 electroanalyzer connected to a Houston Instruments HIPLOT DMP-40 plotter. A saturated calomel electrode (SCE) was used as the reference electrode and was separated from the bulk of the solution by a fritted-glass bridge. Bulk controlled-potential electrolysis was performed with an EG&G Model 173 potentiostat. An EG&G Model 179 X-Y digital coulometer was used to record the current–time curves and the total charge transferred during electrolysis. Thin-layer spectroelectrochemical measurements were performed with an EG&G Model 173 potentiostat which was coupled with a Tracor Northern 6500 rapid-scan spectrometer or with an optical multichannel analyzer, Model ST-1000, from Princeton Instruments, Inc. This latter instrument was used with fiber optics in order to perform spectroelectrochemical experiments in the glovebox. The utilized optically transparent platinum thin-layer electrode (OTTLE) has been described in a previous publication.[21] Low-temperature ESR spectra were measured on a Bruker Model 100D ESR spectrometer. Typical temperatures for these measurements varied between 123 and 153 K.

Results

Electroreduction of (P)Sn. Each (P)Sn derivative exhibits two reversible one-electron reductions and one irreversible two-electron oxidation. The half-wave or peak potentials for these reactions in py, THF, and PhCN containing 0.1 M $(TBA)ClO_4$ or $(TBA)PF_6$ are summarized in Table I, and cyclic voltammograms for reduction and oxidation of (OEP)Sn in each of the three solvents containing 0.1 M $(TBA)ClO_4$ are illustrated in Figure 1. The two reductions in this figure are labeled as reactions I and II, and the oxidation is labeled as reaction III.

The shapes of the current–voltage curves for processes I and II are given by $|E_{pa} - E_{pc}|$ and $|E_p - E_{p/2}| = 65 \pm 5$ mV at a scan rate of 0.1 V/s. Both values are characteristic of a diffusion-controlled one-electron transfer. In addition, the maximum peak current, i_p, is proportional to $v^{1/2}$, indicating the absence of coupled

(1) (a) University of Houston. (b) Université de Bourgogne.
(2) Corwin, A. H.; Collins, O. D. *J. Org. Chem.* **1962**, *27*, 3060.
(3) Guilard, R.; Lecomte, C.; Kadish, K. M. In *Structure and Bonding*; Buchler, J. W., Ed.; Springer-Verlag: Berlin, 1987; Vol. 64 and references therein.
(4) Guilard, R.; Kadish, K. M. *Chem. Rev.* **1988**, *88*, 1121 and references therein.
(5) Kadish, K. M. *Prog. Inorg. Chem.* **1986**, *34*, 435.
(6) Kadish, K. M.; Xu, Q. Y.; Barbe, J.-M.; Anderson, J. E.; Wang, E.; Guilard, R. *Inorg. Chem.* **1988**, *27*, 691.
(7) Guilard, R.; Barbe, J.-M.; Boukhris, A.; Lecomte, C.; Anderson, J. E.; Xu, Q. Y.; Kadish, K. M. *J. Chem. Soc., Dalton Trans.* **1988**, 1109.
(8) Kadish, K. M.; Xu, Q. Y.; Maiya, G. B.; Barbe, J.-M.; Guilard, R. *J. Chem. Soc., Dalton Trans.* **1989**, 1531.
(9) Whitten, D. G.; Yau, J. C.; Carroll, F. A. *J. Am. Chem. Soc.* **1971**, *93*, 2291.
(10) Harel, Y.; Manassen, J. *J. Am. Chem. Soc.* **1977**, *99*, 5817.
(11) Szulbinski, W.; Strojek, J. W. *Inorg. Chim. Acta* **1986**, *118*, 91.
(12) Szulbinski, W.; Zak, J.; Strojek, J. W. *J. Electroanal. Chem. Interfacial Electrochem.* **1987**, *226*, 157.
(13) Crowe, A. J. *Tin Its Uses* **1990**, *162*, 4 and references herein.
(14) Miyamoto, T. K.; Sugita, N.; Matsumoto, Y.; Sasaki, Y.; Konno, M. *Chem. Lett.* **1983**, 1695.
(15) Landrum, J. T.; Amini, M.; Zuckerman, J. J. *Inorg. Chim. Acta* **1984**, *90*, L73.
(16) Felton, R. H.; Linschitz, H. *J. Am. Chem. Soc.* **1966**, *88*, 1113.
(17) Ferguson, J. A.; Meyer, T. J.; Whitten, D. G. *Inorg. Chem.* **1972**, *11*, 2767.
(18) Barbe, J.-M.; Ratti, C.; Richard, P.; Lecomte, C.; Gerardin, R.; Guilard, R. *Inorg. Chem.* **1990**, *29*, 4126.
(19) Guilard, R.; Ratti, C.; Barbe, J.-M.; Dubois, D.; Kadish, K. M. *Inorg. Chem.* **1991**, *30*, 1537.
(20) Kadish, K. M.; Swistak, C.; Boisselier-Cocolios, B.; Barbe, J.-M.; Guilard, R. *Inorg. Chem.* **1986**, *25*, 4336.
(21) Lin, X. Q.; Kadish, K. M. *Anal. Chem.* **1985**, *57*, 1498.

0020-1669/91/1330-4498$02.50/0

Table I. Half-Wave and Peak Potentials (V vs SCE) for the Reduction and Oxidation of (P)Sn in Solvents Containing 0.1 M $(TBA)ClO_4$ or $(TBA)PF_6$

		$(TBA)PF_6$ supporting electrolyte				$(TBA)ClO_4$ supporting electrolyte			
		redn			oxidn	redn			oxidn
porphyrin, P	solvent	$E_{1/2}$	$E_{1/2}$	$\Delta E_{1/2}$, V	E_p^a	$E_{1/2}$	$E_{1/2}$	$\Delta E_{1/2}$, V	E_p^a
TpTP	py	−1.09	−1.48	0.39	0.74	−1.11	−1.51	0.40	0.55
	THF	−1.08	−1.50	0.42	0.68	−1.12	−1.54	0.42	0.62
	PhCN	−1.17	−1.57	0.40	0.56	−1.13	−1.54	0.41	0.59
TmTP	py	−1.08	−1.48	0.40	0.76	−1.09	−1.50	0.41	0.56
	THF	−1.08	−1.50	0.42	0.71	−1.05	−1.47	0.42	0.77
	PhCN	−1.14	−1.56	0.42	0.59	−1.13	−1.55	0.42	0.61
TMP	py	−1.06	−1.60	0.54	0.79	−1.16	−1.71	0.55	0.70
	THF	−1.22	−1.68	0.46	0.73	−1.19	−1.69	0.50	0.86
	PhCN	−1.19	−1.73	0.54	0.62	−1.17	−1.71	0.54	0.63
OEP	py	−1.30	−1.75	0.45	0.60	−1.34	−1.79	0.45	0.48
	THF	−1.28	−1.73	0.45	0.59	−1.26	−1.71	0.45	0.67
	PhCN	−1.40	−1.85	0.45	0.47	−1.37	−1.81	0.44	0.50

[a] Peak potential at a scan rate of 0.1 V/s.

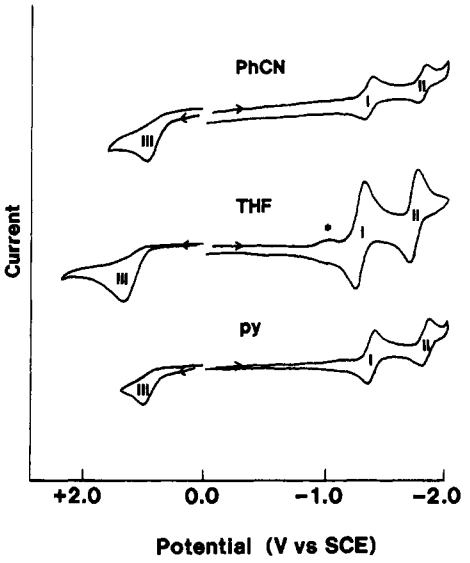

Figure 1. Cyclic voltammograms illustrating the oxidation and reduction of (OEP)Sn in PhCN, THF, and py containing 0.1 M $(TBA)ClO_4$. Scan rate = 0.1 V/s. The starred process is due to a Sn(IV) decomposition product.

chemical reactions on the cyclic voltammetric time scale.

There is only a small dependence of $E_{1/2}$ on supporting electrolyte, and similar potentials are observed for reduction of a given complex in each of the three solvents (see Table I). Half-wave potentials for the two reductions of (P)Sn are separated by an average of 450 mV for the OEP complexes, 410 mV for the TpTP and TmTP complexes, and 520 mV for the TMP complexes. These potential separations are comparable to separations generally observed for other metalloporphyrins which are reduced in two consecutive one-electron reactions at the porphyrin π ring system.[5] Bulk controlled-potential electrolysis of (P)Sn in pyridine containing 0.1 M $(TBA)PF_6$ gives 0.9 ± 0.1 electrons added in the first reduction, and the resulting singly reduced species exhibits a low-temperature ESR spectrum which is centered at $g = 2.003 \pm 0.001$. The coulometric and ESR data are thus self-consistent and indicate the formation of a porphyrin π anion radical in the first one-electron-transfer step.

A summary of UV–visible data for neutral, singly reduced, and singly oxidized (TpTP)Sn and (OEP)Sn in pyridine containing 0.1 M $(TBA)PF_6$ is given in Table II. Each neutral (P)Sn complex exhibits a "hyper" type spectrum. The initial spectra recorded in pyridine containing 0.1 M $(TBA)PF_6$ are identical with those reported in toluene without supporting electrolyte,[18] and this suggests a lack of solvent binding to the metal center of (P)Sn.

The first one-electron reduction of (OEP)Sn in pyridine gives thin-layer spectral changes of the type illustrated in Figure 2a.

Table II. UV–Visible Spectral Data for Neutral, Oxidized, and Reduced (P)Sn in Pyridine Containing 0.1 M $(TBA)PF_6$

	λ_{max}, nm	
redox reacn	(OEP)Sn	(TpTP)Sn
none[a]	386, 497	400, 490, 701
1st redn	386, 453, 519	394, 444, 523
oxidn	406, 539, 575	320, 410,[b] 429, 563, 605

[a] Initial compound. [b] Shoulder.

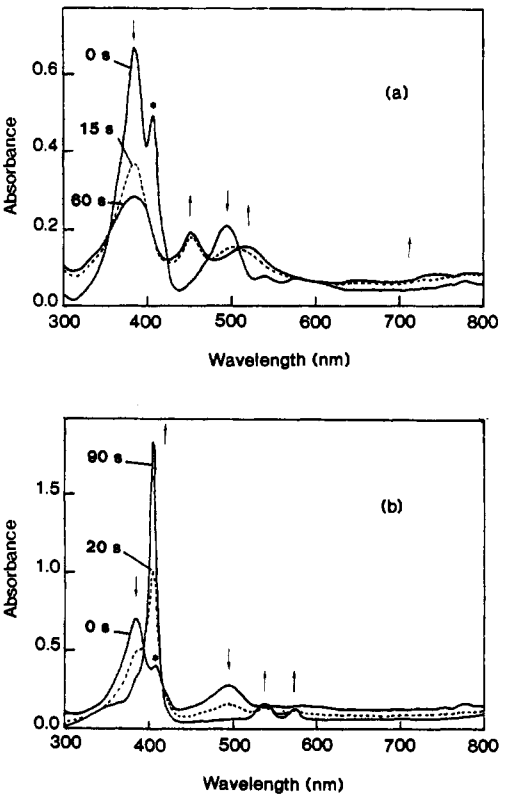

Figure 2. Time-resolved electronic absorption spectra of (OEP)Sn in py containing 0.1 M $(TBA)PF_6$ taken (a) during controlled-potential reduction at −1.6 V and (b) during controlled-potential oxidation at +0.9 V. The starred peaks in the initial (P)Sn spectra are due to small amounts of oxidation products.

The reduction is spectrally reversible, as is also the case for reduction of (TpTP)Sn under the same solution conditions. The spectra of both singly reduced complexes are somewhat atypical in that they exhibit three main bands between 386 and 523 nm. Nevertheless, the overall spectral changes are consistent with formation of a metalloporphyrin π anion radical in the first one-electron-transfer step.

Table III. Half-Wave Potentials (V vs SCE) for Reduction of the Transient and Final Species Produced after Oxidation of (P)Sn in Solvents Containing 0.1 M $(TBA)PF_6$ or $(TBA)ClO_4$

		$(TBA)PF_6$ supporting electrolyte						$(TBA)ClO_4$ supporting electrolyte					
		transient species[a]			final species[b]			transient species[a]			final species[b]		
initial complex	solvent	$E_{1/2}$	$E_{1/2}$	$\Delta E_{1/2}$[c]	$E_{1/2}$	$E_{1/2}$[d]	$\Delta E_{1/2}$[c]	$E_{1/2}$	$E_{1/2}$	$\Delta E_{1/2}$[c]	$E_{1/2}$	$E_{1/2}$[d]	$\Delta E_{1/2}$[c]
(TmTP)Sn	py	−0.20	−0.64	0.44	−0.54	−1.08	0.54	−0.19	−0.60	0.41	−0.57	−1.07	0.50
	THF	−0.14	−0.51	0.37	−0.51	−1.06	0.45	*e*	*e*		−0.45	−1.05	0.60
	PhCN	*e*	*e*		−0.64	−0.97	0.33	*e*	*e*		*f*	*f*	
(TpTP)Sn	py	−0.15	−0.60	0.45	−0.52	−1.09	0.57	−0.23	−0.63	0.40	−0.56	−1.10	0.54
	THF	−0.17	≈−0.5	≈0.3	−0.47	−1.07	0.60	*e*	*e*		−0.51	−1.11	0.60
	PhCN	*e*	*e*		−0.63	−0.96	0.33	*e*	*e*		−0.61	−0.95	0.34
(TMP)Sn	py	−0.08	−0.61	0.55	−0.44	−1.10	0.66	−0.13	−0.60	0.47	−0.54	−1.16	0.62
	THF	≈−0.1	*g*		−0.42	−1.07	0.65	*e*	*e*		−0.41		
	PhCN	*e*	*e*		−0.62	−1.01	0.39	*e*	*e*		−0.61	−1.00	0.39
(OEP)Sn	py	−0.40	−0.85	0.45	−0.75	−1.30	0.55	−0.45	−0.89	0.44	−0.76	−1.33	0.57
	THF	−0.39	−0.77	0.38	−0.69	−1.28	0.59	*e*	*e*		*h*		
	PhCN	*e*	*e*		−0.90	≈−1.2	≈0.3	*e*	*e*		−0.83	−1.17	0.34

[a] First electrogenerated species after oxidation of (P)Sn. [b] Final electrogenerated species after oxidation of (P)Sn. [c] $\Delta E_{1/2}$ = absolute potential difference between first and second reductions (in volts). [d] Values are approximate, since this process (wave V) is merged with wave I (see Table I and Figure 3). [e] Transient not observed at any scan rate up to 50 V/s. [f] Decomposition product of initial complex overlaps with new peak. [g] Peak appears as a shoulder of the process at $E_{1/2}$ = −0.42 V for the final species. [h] Several ill-defined waves are obtained.

Electrooxidation of (P)Sn. Each (P)Sn complex exhibits a single irreversible oxidation. The peak potential for this reaction (labeled process III in Figure 1) varied as a function of the specific porphyrin ring and/or the solvent–supporting electrolyte system and ranged between 0.47 and 0.86 V for a scan rate of 0.1 V/s. Exact peak potentials in py, THF, and PhCN at 0.1 V/s are given in Table I for solutions containing either $(TBA)ClO_4$ or $(TBA)PF_6$ as supporting electrolyte. The peak shape for this oxidation, defined by $|E_p - E_{p/2}|$, varied between 90 and 120 mV (depending upon the complex) and did not change with potential scan rate. However, E_p shifted anodically by 65–87 mV per each 10-fold increase in scan rate.

The broad oxidation peak, the lack of a reduction peak coupled to this process, and the anodic shift of E_p with increase in scan rate are self-consistent and indicate that (P)Sn is oxidized via an initial irreversible (slow) one-electron-transfer reaction. The electrochemical transfer coefficient (αn) for this reaction averaged 0.48, but the exact value depended upon the specific porphyrin macrocycle and/or the solvent–supporting electrolyte system. Also, as expected for this type of process, the oxidation remained irreversible at all temperatures between +22 and −45 °C, as well as at all potential scan rates between 0.02 and 50 V/s.

Several mechanisms can fit the irreversible first step in the overall two-electron oxidation of (P)Sn, and these are E_1E_2C, E_1CE_2, or E_1CE_2C where C is the chemical step (ligation) and E_1 is the initial electron-transfer process, which is rate controlling. The αn of 0.48 is consistent with formation of a Sn(III) intermediate, but this species is too short-lived to be observed, and only the overall Sn(II)/Sn(IV) process can be monitored.

UV–visible spectra obtained during controlled-potential oxidation of (P)Sn in a thin-layer cell are discussed in the following section and indicate the ultimate generation of a Sn(IV) porphyrin product. Only one electroactive species is detected in PhCN, but two different products are observed in pyridine or THF. An example of the resulting cyclic voltammograms for the oxidation and reduction of (TmTP)Sn in pyridine is given in Figure 3. The upper three voltammograms were obtained by using an initial negative potential scan between 0.0 and −2.0 V, while the lower three were obtained by using an initial positive scan between 0.0 and +1.0 V, followed by a negative potential scan to −2.0 V. In this manner, the upper three voltammograms show reductions due only to the initial (TmTP)Sn complex, while the lower three have reduction peaks which can be assigned to both the initial metalloporphyrin (reactions I and II) and the products of the (TmTP)Sn electrooxidation (reactions IV, V, IV′, and V′).

One of the products of (TmTP)Sn oxidation in pyridine containing 0.1 M $(TBA)PF_6$ is reduced at $E_{1/2}$ = −0.20 and −0.64 V and is only observed at high potential scan rates. A second product is reduced at $E_{1/2}$ = −0.54 and −1.08 V, and these peaks are observed at low potential scan rates. Similar sets of two

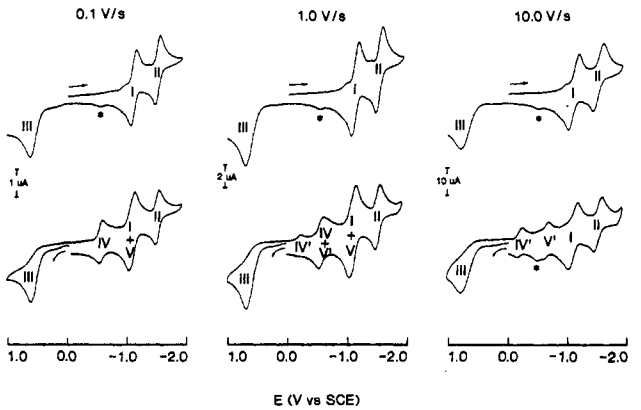

Figure 3. Cyclic voltammograms of (TmTP)Sn in py containing 0.1 M $(TBA)PF_6$ at scan rates of 0.1, 1.0, and 10.0 V/s. The upper three voltammograms were obtained with an initial negative scan between 0.0 and −2.0 V, while the lower three were measured by using an initial positive sweep from 0.0 to +1.0 V. The starred peaks are due to decomposition products, which appear after the second reduction.

reduction processes were observed for each of the four investigated complexes in pyridine containing $(TBA)PF_6$ or $(TBA)ClO_4$ supporting electrolyte as well as in THF containing $(TBA)PF_6$. The specific scan rate at which the two sets of peaks start to appear or disappear depended upon the porphyrin macrocycle and/or the solvent–supporting electrolyte system and varied over the range 1–50 V/s.

Only one electroactive species could be monitored after oxidation of (P)Sn in PhCN or THF containing 0.1 M $(TBA)ClO_4$, and potentials for reduction of this complex are similar to those for reduction of the species formed as a final electrooxidation product in pyridine or THF containing 0.1 M $(TBA)PF_6$. Values of $E_{1/2}$ for both sets of electrode reactions in the six investigated solvent–supporting electrolyte systems are summarized in Table III.

Coulometric measurements performed during bulk controlled-potential oxidation of (P)Sn in pyridine containing 0.1 M $(TBA)PF_6$ give an irreproducible number of electrons transferred, which ranged from 1.0 to 2.0 electrons per molecule. The overall oxidation proceeds slowly, and consistent with the electrochemical irreversibility of this reaction, no reverse current is observed when a potential of 0.0 V is applied at the completion of the oxidation. As expected, the oxidations of (TpTP)Sn and (OEP)Sn are both spectrally irreversible and the thin-layer spectra of the final electrooxidized species are similar to UV–visible spectra reported for unreduced $[(P)Sn(ClO_4)(THF)]^+$ in THF[8] or for unreduced $(P)Sn(ClO_4)_2$ in pyridine containing 0.1 M $(TBA)PF_6$ as supporting electrolyte. An example of this spectrum is shown in

Scheme I

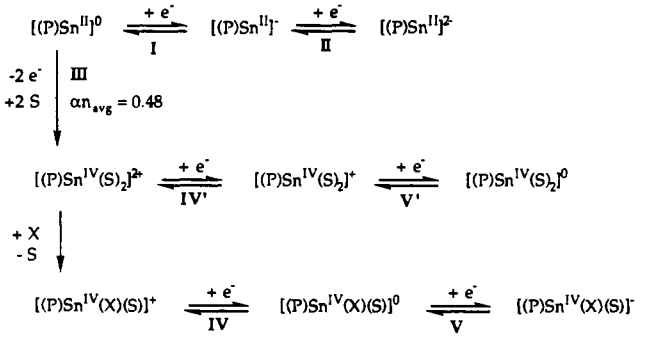

Figure 2b for the OEP complex.

Discussion

The resulting spectroscopic and electrochemical data are consistent with the overall oxidation/reduction mechanism given in Scheme I, where S represents the solvent, X = PF_6^- or ClO_4^-, and the electrode reactions with Roman numerals are as noted in Figure 3.

The initial two reductions of (P)Sn (reactions I and II) are reversible diffusion-controlled processes which generate porphyrin π anion radicals and dianions. In contrast, the oxidation of (P)Sn (reaction III) is electrochemically irreversible (slow) and proceeds via an overall two-electron transfer to stepwise generate two different Sn(IV) porphyrins in solution. Both Sn(IV) products are observed by cyclic voltammetry in py or THF containing 0.1 M $(TBA)PF_6$, and this is illustrated in Figure 3 for the case of (TmTP)Sn in pyridine.

The transient species observed in pyridine or THF containing 0.1 M $(TBA)PF_6$ is assigned as $[(P)Sn^{IV}(S)_2]^{2+}$ (S = py or THF). This species is not seen in THF containing 0.1 M $(TBA)ClO_4$, and this can be reasonably explained by the fact that THF has weaker coordinating properties than pyridine while ClO_4^- is a stronger ligand than PF_6^-. This would lead to a more rapid displacement of THF from $[(P)Sn(THF)_2]^{2+}$ to form $[(P)Sn(ClO_4)(THF)]^+$ as a final observed electrooxidation product in the $(TBA)ClO_4$ solution. A transient electroactive species is also not seen in PhCN containing either $(TBA)ClO_4$ or $(TBA)PF_6$. Again, this can be accounted for by the poor coordinating ability of PhCN, which is less likely to stabilize a bis-solvated tin(IV) porphyrin complex in the presence of ClO_4^- or PF_6^- counterions.

The electrochemical data indicate formation of similar final (P)Sn oxidation products in all three solvents, and these species are assigned as $[(P)Sn^{IV}(X)(S)]^+$ where S = py, PhCN, or THF and X = PF_6^- or ClO_4^-. Both the transient and final electrogenerated Sn(IV) porphyrins undergo two reductions, and these are postulated to occur at the porphyrin π ring system.

The assignment of $[(P)Sn^{IV}(S)_2]^{2+}$ and $[(P)Sn^{IV}(X)(S)]^+$ as stepwise (P)Sn oxidation products comes from spectroscopic and electrochemical data for $(P)Sn(ClO_4)_2$ in THF[8] as well as from UV–visible and electrochemical data obtained in this present study for oxidation of (P)Sn in py, THF, or PhCN. $(P)Sn(ClO_4)_2$ exists in its dissociated $[(P)Sn(ClO_4)(THF)]^+$ form in THF containing 0.1 M $(TBA)ClO_4$.[8] A dissociated form of the complex also exists in pyridine. The UV–visible spectrum of $(P)Sn(ClO_4)_2$ exhibits bands at 430, 564, and 605 nm (P = TpTP) or 406, 538, and 575 nm (P = OEP) in pyridine containing 0.1 M $(TBA)PF_6$. These spectra are virtually identical with those obtained after oxidation of the (TpTP)Sn or (OEP)Sn derivative in pyridine containing 0.1 M $(TBA)PF_6$ (see Table II and Figure 2b), and the spectra under these latter conditions are therefore assigned as those of $[(P)Sn(PF_6)(py)]^+$.

The peak potentials for the irreversible oxidation of $(P)Sn^{II}$ (0.47–0.86 V vs SCE at a scan rate of 0.1 V/s) are similar to values of E_p for the irreversible oxidation of the Sn(IV) porphyrin chalcogen derivatives under the same experimental conditions.[19] This is perhaps interesting, but it should be noted that the Sn(IV) compounds are oxidized at the axial ligand while (P)Sn is oxidized at the central metal.[22]

It should also be noted that the potentials for electroreduction of $[(P)Sn(X)(S)]^+$ are similar in each solvent–supporting electrolyte mixture and these potentials are also similar to $E_{1/2}$ values for reduction of $[(P)Sn(ClO_4)(THF)]^+$ in THF[8] containing 0.1 M $(TBA)ClO_4$. These values are all about 350 mV more negative than potentials for reduction of the transient electrogenerated $[(P)Sn(S)_2]^{2+}$ complex in py or THF (processes IV′ and V′). This result agrees with data for $(P)Sn(OH)_2$,[8,23] $(P)Sn(F)_2$,[8,23] and $[(P)Sn(ClO_4)(THF)]^+$,[8] the first two of which exist as undissociated complexes in nonaqueous media and are therefore more difficult to reduce than the singly charged dissociated species by ~350 mV. The trends in $E_{1/2}$ for the first reduction of (P)Sn (peak I), $[(P)Sn(X)(S)]^+$ (X = PF_6^- or ClO_4^-) (peak IV), and $[(P)Sn(S)_2]^{2+}$ (peak IV′) in Tables I and III are thus self-consistent with respect to the relationship between $E_{1/2}$ for electroreduction and the overall charge of the reactive complex. Similarly, $E_{1/2}$ values for reduction of $(P)Sn^{II}$ are more negative than $E_{1/2}$ for reduction of $(P)Sn^{IV}$ complexes such as (P)SnS,[19] (P)SnSe,[19] $(P)Sn(OH)_2$,[8,23] or $(P)SnF_2$.[8,23] This trend is consistent with the increased electron density at the metal center upon going from the Sn(IV) to the Sn(II) derivatives.

Acknowledgment. The support of the CNRS and of the National Science Foundation (Grants CHE-8822881 and INT-8413696) is gratefully acknowledged.

Registry No. $[(TpTP)Sn^{II}]$, 129390-30-3; $[(TmTP)Sn^{II}]$, 129390-29-0; $[(TMP)Sn^{II}]$, 129390-31-4; $[(OEP)Sn^{II}]$, 129390-32-5; $[(TpTP)Sn^{II}]^-$, 136659-01-3; $[(TmTP)Sn^{II}]^-$, 136659-02-4; $[(TMP)Sn^{II}]^-$, 136659-03-5; $[(OEP)Sn^{II}]^-$, 136659-04-6; $[(TpTP)Sn^{II}]^{2-}$, 136659-05-7; $[(TmTP)Sn^{II}]^{2-}$, 136659-06-8; $[(TMP)Sn^{II}]^{2-}$, 136659-07-9; $[(OEP)Sn^{II}]^{2-}$, 136659-08-0; $[(TpTP)Sn^{II}(PF_6)(Py)]^+$, 136659-09-1; $[(TpTP)Sn^{IV}(PF_6)(THF)]^+$, 136659-10-4; $[(TpTP)Sn^{IV}(PF_6)(PhCN)]^+$, 136659-11-5; $[(TmTP)Sn^{IV}(PF_6)(Py)]^+$, 136659-12-6; $[(TmTP)Sn^{IV}(PF_6)(THF)]^+$, 136659-13-7; $[(TmTP)Sn^{IV}(PF_6)(PhCN)]^+$, 136659-14-8; $[(TMP)Sn^{IV}(PF_6)(Py)]^+$, 136659-15-9; $[(TMP)Sn^{IV}(PF_6)(THF)]^+$, 136659-16-0; $[(TMP)Sn^{IV}(PF_6)(PhCN)]^+$, 136659-17-1; $[(OEP)Sn^{IV}(PF_6)(Py)]^+$, 136659-18-2; $[(OEP)Sn^{IV}(PF_6)(THF)]^+$, 136659-19-3; $[(OEP)Sn^{IV}(PF_6)(PhCN)]^+$, 136659-20-6; $[(TpTP)Sn^{IV}(ClO_4)(Py)]^+$, 136659-21-7; $[(TpTP)Sn^{IV}(ClO_4)(THF)]^+$, 122202-68-0; $[(TpTP)Sn^{IV}(ClO_4)(PhCN)]^+$, 136659-22-8; $[(TmTP)Sn^{IV}(ClO_4)(Py)]^+$, 136659-23-9; $[(TmTP)Sn^{IV}(ClO_4)(THF)]^+$, 122202-70-4; $[(TmTP)Sn^{IV}(ClO_4)(PhCN)]^+$, 136659-24-0; $[(TMP)Sn^{IV}(ClO_4)(Py)]^+$, 136659-25-1; $[(TMP)Sn^{IV}(ClO_4)(THF)]^+$, 136659-26-2; $[(TMP)Sn^{IV}(ClO_4)(PhCN)]^+$, 136659-27-3; $[(OEP)Sn^{IV}(ClO_4)(Py)]^+$, 136659-28-4; $[(OEP)Sn^{IV}(ClO_4)(THF)]^+$, 136659-29-5; $[(OEP)Sn^{IV}(ClO_4)(PhCN)]^+$, 136659-30-8; Py, 110-86-1; THF, 109-99-9; PhCN, 100-47-0; $(Bu)_4N^+ \cdot PF_6^-$, 3109-63-5; $(Bu)_4N^+ \cdot ClO_4^-$, 1923-70-2.

(22) The porphyrin literature contains numerous examples where two complexes have the same central metal ion and similar potentials but different sites of electron transfer. A good example to illustrate this point involves (TPP)Fe(NO) and $(TPP)Fe(C_6H_5)$ both of which are oxidized at 0.54–0.57 V in CH_2Cl_2. The first reaction is that for Fe^{II}/Fe^{III}, while the second is that for Fe^{III}/Fe^{IV} (see ref 5).

(23) Half-wave potentials in CH_2Cl_2 containing 0.1 M $(TBA)ClO_4$ as measured vs SCE in our laboratory are as follows. $(TmTP)Sn(OH)_2$: −0.97, −1.35 V (−0.81, −1.21 V in py containing 0.1 M $(TBA)PF_6$). $(TpTP)SnF_2$: −0.87, −1.29 V. $(TmTP)SnF_2$: −0.87, −1.27 V. $(TpTP)SnCl_2$: −0.83, −1.20 V.